

Published in final edited form as:

*Inorg Chem.* 2010 November 15; 49(22): 10226–10228. doi:10.1021/ic101700t.

## Illuminating Metal Ion Sensors – Benzimidazolesulfonamide Metal Complexes

David Martin, Matthieu Rouffet, and Seth M. Cohen

Dept. of Chemistry and Biochemistry, University of California, San Diego, La Jolla, CA 92093

### Abstract

The synthesis, structure, and solution spectroscopy of several 2-sulfonamidophenylbenzimidazole metal complexes is reported. These ligands, which have been reported as selective molecular sensors for  $Zn^{2+}$ , readily form complexes with  $Co^{2+}$ ,  $Ni^{2+}$ ,  $Cu^{2+}$ , and  $Zn^{2+}$ . Surprisingly, the ligand adopts different binding modes depending on the metal ion. The work here provides insight into the coordination chemistry of these ligands that may allow for the development of improved metal ion sensors and metalloprotein inhibitors.

Despite much effort in trying to unravel the role of metal ions in biology, much remains to be learned about how metal cations are trafficked and stored prior to their incorporation into different metalloproteins.<sup>1</sup> Of particular interest is zinc, which is the second most abundant d-block metal ion in humans.<sup>2</sup> Historically,  $Zn^{2+}$  was detected using dithizone as a histochemical stain (Chart 1),<sup>1</sup> which revealed much about the spatial distribution of  $Zn^{2+}$  in various tissues. Today, fluorescent probes have attracted considerable attention for the direct visualization of biological  $Zn^{2+}$  at the molecular level. One of the first probes to be used was 8-hydroxyquinoline, which was further developed into Zinquin<sup>3</sup>·4 (Chart 1), a compound containing an 8-sulfonamidoquinoline core. The metal binding properties and coordination chemistry of the 8-sulfonamidoquinoline motif has been well described in the literature. These compounds were found to show a strong increase in fluorescence upon binding  $Zn^{2+}$ . Later, Fahrni et al. developed  $Zn^{2+}$ -selective fluorescent sensors based on 2-(2'-tosylaminophenyl)benzimidazole (TPBI, Chart 1).<sup>5</sup> These molecules absorb at ~300–340 nm and emit at ~400 nm (upon  $Zn^{2+}$  coordination), which may limit their use in vivo; however they are attractive because they provide a ratiometric response, which allows for the quantitative analysis of  $Zn^{2+}$ .<sup>5</sup>

In addition to  $Zn^{2+}$ -specific fluorescent probes, our laboratory has recently described the use of these zinc binding motifs in the design of matrix metalloproteinase (MMP) inhibitors.<sup>6</sup> It was found that several 8-sulfonamidoquinoline and 2-sulfonamidophenylbenzimidazole fragments showed good activity and selectivity against several MMP isoforms. Despite the importance of metal binding in the activity of these compounds, there is essentially no information on the coordination chemistry of 2-sulfonamidophenylbenzimidazole ligands to any metal ion. In this study, several benzimidazole sulfonamide metal complexes are reported and their binding modes are directly compared to the well-documented 8-sulfonamidoquinoline analogues.

Correspondence to: Seth M. Cohen.

Supporting Information Available: Synthetic and crystallographic details, Table S1. This material is available free of charge via the Internet at <http://pubs.acs.org>. X-ray crystallographic files in CIF format are available free of charge via the Internet at <http://www.ccdc.cam.ac.uk>. Refer to CCDC reference numbers 789121-4.

The TPBI ligand readily forms a variety of metal complexes under mild conditions.  $\text{Co}^{2+}$ ,  $\text{Ni}^{2+}$ , and  $\text{Zn}^{2+}$  complexes were obtained by combining methanolic solutions of TPBI and a metal salt at room temperature. In the preparation of  $\text{Ni}^{2+}$  and  $\text{Zn}^{2+}$  complexes the metal acetate salts were used and precipitation of the complexes was observed immediately. In the case of  $\text{Co}^{2+}$ , the nitrate salt was used necessitating the addition of base ( $\text{Et}_3\text{N}$ ) for complex formation. To synthesize the  $\text{Cu}^{2+}$  complex, a methanolic TPBI solution was added to a yellow solution of  $\text{CuCl}_2 \cdot 2\text{H}_2\text{O}$  in acetonitrile. Upon addition of aqueous  $\text{NaOH}$  the solution turned dark red, indicating formation of the complex. This  $\text{Cu}^{2+}$  complex did not precipitate out of the reaction mixture, so the solvents were removed under vacuum and the resulting residue dissolved in acetone/ $\text{CH}_2\text{Cl}_2$ . The product was crystallized by vapor diffusion with diethyl ether as the precipitant.

UV-Vis absorption spectra for the complexes are shown in Figure 1. In the UV region,  $\text{Zn}(\text{TPBI})_2$  has an absorbance maxima at 296 nm ( $\epsilon = 29,000 \text{ M}^{-1}\text{cm}^{-1}$ ), 304 nm ( $\epsilon = 35,000 \text{ M}^{-1}\text{cm}^{-1}$ ), and 334 nm ( $\epsilon = 32,000 \text{ M}^{-1}\text{cm}^{-1}$ ). The  $\text{Co}^{2+}$  and  $\text{Ni}^{2+}$  complexes also show maxima at 296 and 304 nm ( $\text{Co}(\text{TPBI})_2$ :  $\epsilon = 33,000$  and  $37,000 \text{ M}^{-1}\text{cm}^{-1}$ ;  $\text{Ni}(\text{TPBI})_2$ :  $\epsilon = 31,000$  and  $34,000 \text{ M}^{-1}\text{cm}^{-1}$ ). In addition,  $\text{Co}(\text{TPBI})_2$  displays a transition at 338 nm and  $\text{Ni}(\text{TPBI})_2$  at 352 nm ( $\epsilon = 30,000 \text{ M}^{-1}\text{cm}^{-1}$  in both cases).  $\text{Cu}(\text{TPBI})\text{Cl}$  shows only one transition at 296 nm ( $\epsilon = 19,000 \text{ M}^{-1}\text{cm}^{-1}$ ). The complexes are relatively weakly colored, as shown by their absorbance in the visible region of the spectrum. The red  $\text{Co}(\text{TPBI})_2$  complex is the most intensely colored, with maxima at 532 and 550 nm and extinction coefficients of 237 and  $231 \text{ M}^{-1}\text{cm}^{-1}$ , respectively.  $\text{Co}(\text{TPBI})_2$  also has a weak, broad absorbance centered at 790 nm ( $\epsilon = 37 \text{ M}^{-1}\text{cm}^{-1}$ ).  $\text{Cu}(\text{TPBI})\text{Cl}$  is also red, having an absorbance maximum at 510 nm ( $\epsilon = 161 \text{ M}^{-1}\text{cm}^{-1}$ ) and a very broad absorbance centered at 840 nm ( $\epsilon = 95 \text{ M}^{-1}\text{cm}^{-1}$ ) that trails into the visible region. The green  $\text{Ni}(\text{TPBI})_2$  complex has the faintest color, with absorbance maxima at 448 and 690 nm ( $\epsilon = 109$  and  $55 \text{ M}^{-1}\text{cm}^{-1}$ , respectively). The fluorescence of the complexes was checked using a hand-held UV lamp (254 and 365 nm), and only  $\text{Zn}(\text{TPBI})_2$  emitted.  $\text{Zn}(\text{TPBI})_2$  was a strong emitter in aqueous solution at  $\sim 415 \text{ nm}$  when excited at 305 nm (data not shown).<sup>5</sup>

Single-crystals of  $\text{M}(\text{TPBI})_2$  ( $\text{M} = \text{Zn}^{2+}$ ,  $\text{Co}^{2+}$ ,  $\text{Ni}^{2+}$ ) and  $\text{Cu}(\text{TPBI})\text{Cl}$  were obtained and their structures were determined by X-ray diffraction. Colorless blocks of  $\text{Zn}(\text{TPBI})_2 \cdot 2\text{CHCl}_3$  crystallize in the monoclinic space group  $C2/c$ . The asymmetric unit consists of a deprotonated TPBI ligand bound by the imidazole and sulfonamide nitrogen atoms to a  $\text{Zn}^{2+}$  ion with bond lengths of 2.005(2) and 1.978(2) Å, respectively (Figure 2). The complex co-crystallized with one  $\text{CHCl}_3$  solvent molecule in the asymmetric unit. Extension of the inversion symmetry reveals a heavily disordered tetrahedral  $\text{ZnN}_4$  coordination sphere with N-Zn-N angles ranging from  $92.05(7)^\circ$  to  $133.2(1)^\circ$ . A long interaction between the  $\text{Zn}^{2+}$  ion and one of the sulfonamide oxygen atoms may contribute to this distortion (Zn-O  $\sim 2.70$  Å).

Red and green blocks of  $\text{Co}(\text{TPBI})_2 \cdot 2\text{DMF}$  and  $\text{Ni}(\text{TPBI})_2 \cdot 2\text{DMF}$  also crystallized in the space group  $C2/c$  with a similar asymmetric unit to that of  $\text{Zn}(\text{TPBI})_2$ , but with the  $\text{CHCl}_3$  solvent replaced by a DMF molecule. The TPBI ligand adopts a similar binding mode as in the  $\text{Zn}^{2+}$  complex (Figure 2). In  $\text{Co}(\text{TPBI})_2$ , the Co-N distances are 1.981(3) and 1.992(3) Å for the sulfonamide and imidazole nitrogens, respectively. The tetrahedral  $\text{CoN}_4$  coordination is more distorted than in the  $\text{Zn}^{2+}$  complex, with N-Co-N angles ranging from  $91.5(1)^\circ$  to  $138.5(2)^\circ$ . This increase in distortion is accompanied by a closer interaction between the Co atom and sulfonamide oxygen atoms, with a Co-O bond length of 2.62 Å (Figure 2). The Ni-N bonds in  $\text{Ni}(\text{TPBI})_2$  are somewhat shorter at 1.962(2) and 1.981(2) Å for the sulfonamide and imidazole nitrogen atoms, respectively. The  $\text{NiN}_4$  tetrahedron is even more distorted, having angles between  $91.13(9)^\circ$  and  $143.68(14)^\circ$  and a strong interaction with the sulfonamide oxygen atoms with a Ni-O distance of 2.57 Å.

Red blocks of Cu(TPBI)Cl crystallize in the triclinic space group  $P\bar{1}$  with an asymmetric unit consisting of one  $\text{Cu}^{2+}$  ion bound by a single deprotonated TPBI ligand and a chloride ion (Figure 3). The  $\text{Cu}^{2+}$  ion adopts a distorted square planar geometry consisting of the chloride ion, imidazole and sulfonamide nitrogen atoms, and unlike the previous structures, a fully coordinated sulfonamide oxygen atom. The Cu-N distances are much shorter than the M-N bonds in the other structures at 1.956(3) and 1.908(3) Å for the imidazole and sulfonamide nitrogen atoms, respectively. The Cu-O distance is 2.235(2) Å and the Cu-Cl distance is 2.214(1) Å. The  $\text{Cu}^{2+}$  ion is coplanar with the Cl and N donors, with the oxygen donor 17.6° out of the plane as measured by the N-N-Cl-O torsion angle. Attempts to make a homoleptic Cu(TPBI)<sub>2</sub> complex with other metal sources such as nitrate, acetate, sulfate, and acetylacetonate were unsuccessful.

The primary structural difference between the TPBI and the well-studied quinoline sulfonamide ligands (of the type used in Zinquin, Chart 1) is that upon metal binding, the TPBI forms a six-member chelate as opposed to a five-membered ring for the quinoline-based ligands. This causes the bite distance ( $N_{\text{benz}}-N_{\text{amide}}$ ) to be ~0.2 Å larger, yielding  $N_{\text{benz}}-M-N_{\text{amide}}$  bond angles that are roughly 10° wider than those in the 8-sulfonamidoquinoline complexes. The other consequence of the six-member chelate is the closer positioning of the sulfonamide functionality to the metal, as observed by the  $N_{\text{benz/quin}}-N_{\text{amide}}-S$  angle (~170° for quinoline-based complexes compared to 150° for TPBI). Angling of the sulfonamide group toward the metal allows one of the oxygen atoms to act as a weak donor, which is a feature not found in the structures of analogous quinoline-based complexes.<sup>3, 7-23</sup>

Many homoleptic complexes of quinolinesulfonamide ligands with  $\text{Zn}^{2+}$  and  $\text{Cu}^{2+}$  have been previously reported. The  $\text{Zn}^{2+}$  complexes do not differ significantly from the TPBI complex reported here, aside from those differences described above.<sup>3, 8, 11, 12, 14, 15, 23</sup> In the case of  $\text{Cu}^{2+}$ , the ability of the TPBI ligand to supply a third donor deters the formation of a homoleptic complex as found in previously reported structures with 8-sulfonamidoquinoline ligands.<sup>9, 10, 13, 16-20</sup> The metal adopts the favored square planar geometry and avoids steric clashes between ligands by retaining a chloride ligand as its fourth donor. The more electron-deficient  $\text{Co}^{2+}$  and  $\text{Ni}^{2+}$  have complexes reported with two quinoline sulfonamide ligands, but the metals also ligate two solvent molecules (water or methanol) in order to adopt octahedral geometry.<sup>7, 21</sup> Homoleptic complexes have only been reported by using bulkier 2,4-dimethylquinoline<sup>22</sup> and dimethylaminonaphthalene<sup>24</sup> sulfonamide ligands in order to deter the ligation of solvent molecules. In contrast, the TPBI ligand readily makes homoleptic complexes with these metals with donation from sulfonamide oxygen atoms and the somewhat bulkier ligand framework. 2-(2,2-Sulfonamidophenyl)benzimidazole derivatives are promising fluorescence-based sensors for  $\text{Zn}^{2+}$  as well as potent leads for metalloproteinase inhibitors. The detailed coordination chemistry provided here will be essential to developing the next generation of sensors and inhibitors based on these scaffolds.

## Supplementary Material

Refer to Web version on PubMed Central for supplementary material.

## Acknowledgments

We thank Dr. Y. Su for performing the mass spectrometry experiments. This work was supported by the NIH (R21HL094571-01).

## References

1. McRae R, Bagchi P, Sumalekshmy S, Fahrni CJ. *Chem Rev.* 2009; 109:4780–4827. [PubMed: 19772288]
2. Nolan EM, Lippard SJ. *Acc Chem Res.* 2008; 42:193–203. [PubMed: 18989940]
3. Nasir MS, Fahrni CJ, Suhy DA, Kolodsick KJ, Singer CP, O'Halloran TV. *J Biol Inorg Chem.* 1999; 4:775–783. [PubMed: 10631609]
4. Fahrni CJ, O'Halloran TV. *J Am Chem Soc.* 1999; 121:11448–11458.
5. Henary MM, Wu Y, Fahrni CJ. *Chem Eur J.* 2004; 10:30153025.
6. Rouffet M, de Oliveira CAF, Udi Y, Agrawal A, Sagi I, McCammon JA, Cohen SM. *J Am Chem Soc.* 2010; 132:8232–8233. [PubMed: 20507095]
7. Castresana JM, Elizalde MP, Arrieta JM, Germain G, Declercq JP. *Acta Cryst Sect C.* 1984; 40:763–765.
8. da Silva LE, Joussef AC, Foro S, Schmidt B. *Acta Cryst Sect E.* 2006; 62:m1258–m1259.
9. da Silva LE, Joussef AC, Foro S, Schmidt B. *Acta Cryst Sect E.* 2006; 62:m912–m913.
10. da Silva LE, Joussef AC, Foro S, Schmidt B. *Acta Cryst Sect E.* 2006; 62:m518–m519.
11. da Silva LE, Joussef AC, Foro S, Schmidt B. *Acta Cryst Sect E.* 2006; 62:m516–m517.
12. da Silva LE, Joussef AC, Foro S, Schmidt B. *Acta Cryst Sect E.* 2006; 62:m1901–m1903.
13. da Silva LE, Joussef AC, Foro S, Schmidt B. *Acta Cryst Sect E.* 2006; 62:m1606–m1608.
14. da Silva LE, Joussef AC, Foro S, Schmidt B. *Acta Cryst Sect E.* 2006; 62:m1773–m1775.
15. da Silva LE, Joussef AC, Foro S, Schmidt B. *Acta Cryst Sect E.* 2006; 62:m1719–m1721.
16. Lim MH, Lippard SJ. *Inorg Chem.* 2006; 45:8980–8989. [PubMed: 17054358]
17. Macías B, Villa MV, García I, Castiñeiras A, Borrás J, Cejudo-Marin R. *Inorg Chim Acta.* 2003; 342:241–246.
18. Qiu L, Jiang P, He W, Tu C, Lin J, Li Y, Gao X, Guo Z. *Inorg Chim Acta.* 2007; 360:431–438.
19. Macías B, Villa MV, Fiz E, García I, Castiñeiras A, Gonzalez-Alvarez M, Borrás J. *J Inorg Biochem.* 2002; 88:101–107. [PubMed: 11750031]
20. Macías B, Villa MV, Gómez B, Borrás J, Alzuet G, González-Álvarez M, Castiñeiras A. *J Inorg Biochem.* 2007; 101:444–451. [PubMed: 17222455]
21. Macías B, García I, Villa MV, Borrás J, Castiñeiras A, Sanz F. *Polyhedron.* 2002; 21:1229–1234.
22. Fomina IG, Sidorov AA, Aleksandrov GG, Mikhailova TB, Pakhmutova EV, Novotortsev VM, Ikorskii VN, Eremenko IL. *Russ Chem Bull.* 2004; 53:1477–1487.
23. Macías B, García I, Villa MV, Borrás J, Castiñeiras A, Sanz F. *Z Anorg Allg Chem.* 2003; 629:255–260.
24. Lim MH, Kuang C, Lippard SJ. *Chem BioChem.* 2006; 7:1571–1576.

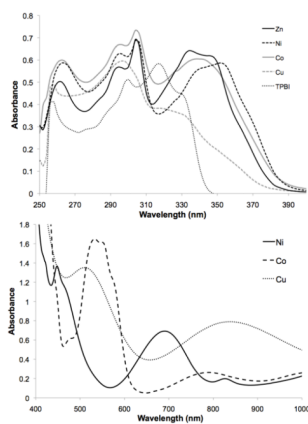


**Figure 1.** *Top:* Representative UV absorbance spectra of TPBI and its complexes; *Bottom:* Visible absorbance spectra of Ni(TPBI)<sub>2</sub>, Co(TPBI)<sub>2</sub>, and Cu(TPBI)Cl. All spectra were recorded in DMSO.

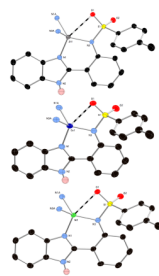


**Figure 2.** Asymmetric units of Zn-(top), Co-(middle) and Ni(TPBI)<sub>2</sub> (bottom) with solvent molecules and hydrogen atoms (except for the imidazole N-H) removed for clarity. Thermal ellipsoids are shown at 50% probability.

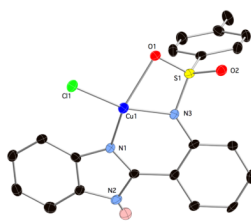


**Figure 3.** Asymmetric unit of Cu(TPBI)Cl with hydrogen atoms (except for the imidazole N-H) removed for clarity. Thermal ellipsoids are shown at 50% probability.

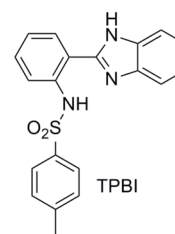
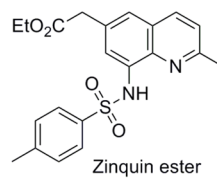
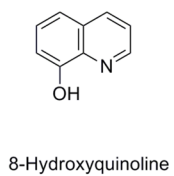


**Chart 1.**  
Compounds used as stains and sensors for Zn<sup>2+</sup>.